Supplement of Atmos. Chem. Phys., 22, 4339–4353, 2022
https://doi.org/10.5194/acp-22-4339-2022-supplement


Atmospheric Chemistry and Physics
Open Access

*Supplement of*

# Seasonal characteristics of atmospheric peroxyacetyl nitrate (PAN) in a coastal city of Southeast China: Explanatory factors and photochemical effects

**Taotao Liu et al.**

*Correspondence to:* Jinsheng Chen (jschen@iue.ac.cn) and Youwei Hong (ywhong@iue.ac.cn)

# Captions:

**Text 1.** Model Validation.

**Figure S1.** Residual test results of the Generalized Additive Model (GAM) in spring.

**Figure S2.** Residual test results of the Generalized Additive Model (GAM) in autumn.

**Figure S3.** Scatter plots of PAN versus $O_3$ during the observation periods.

**Figure S4.** Wind direction frequency and wind speed plots in (a) spring and (b) autumn during the observation periods.

**Figure S5.** Bivariate plot of PAN maxing ratios in (a) spring and (b) autumn, and $O_3$ mixing ratios in (c) spring and (d) autumn, respectively (units: ppbv of PAN and $O_3$ maxing ratio, $m \cdot s^{-1}$ of wind speed).

**Figure S6.** Response curves (autumn) in the multiple-factor model of PAN mixing ratio to changes in (a) NO, (b) Ox ($Ox=O_3+NO_2$), (c) TVOCs, (d) $PM_{2.5}$ concentration, (e) ultraviolet radiation (UV), (f) air temperature (T), (g) relative humidity (RH), and (h) wind speed (WS). The y-axis is the smoothing function values. For example, s(NO, df) shows the trend in PAN when NOchanges, and the number of df is the degree of freedom. The x-axis is the influencing factor, and the shaded area around the solid blue line indicates the 95% confidence interval of PAN. The blue vertical short lines represent the distribution characteristics of the explanatory variables (units: NO (ppbv), Ox ($O_3+NO_2$) (ppbv), TVOCs (ppbv), $PM_{2.5}$ ($\mu g \cdot m^{-3}$), UV ($W \cdot m^{-2}$), T (°C), RH (%), WS ($m \cdot s^{-1}$)).

**Figure S7.** The OBM-MCM calculated relative incremental reactivity (RIR) for major $O_3$ precursor groups in (a) spring and (b) autumn during the daytime (06:00-17:00 LT) on different pollution scenarios.

**Figure S8.** Diurnal trends of the relative variations of $O_3$ net production $\triangle P(O_3)$ ($ppbv \cdot h^{-1}$) during the daytime in the SC1 to those simulated with PAN chemistry disabled in SC2 during the daytime (06:00-17:00) in (a) spring and (b) autumn (unit: $ppbv \cdot h^{-1}$ for $\triangle P(O_3)$). The data in the picture came from the days that have significant promotion effects of PAN on $O_3$ in spring and autumn.

**Figure S9.** Response curves (spring) of $\triangle P(O_3)$ to changes in (a) $\triangle$ROx, (b) ultraviolet radiation (UV), (f) air temperature (T), (g) relative humidity (RH), and (h) wind speed (WS). The y-axis is the smoothing function values. For example, s(UV, df) shows the trend in $\triangle P(O_3)$ when UV changes, and the number of df is the degree of freedom. The x-axis is the influencing factor, and the shaded area around the solid blue line indicates the 95% confidence interval of $\triangle P(O_3)$. The blue vertical short lines represent the distribution characteristics of the explanatory variables (units: $\triangle$ROx ($molecules \cdot cm^{-3}$), UV ($W \cdot m^{-2}$)).

**Figure S10.** Response curves (autumn) of $\triangle P(O_3)$ to changes in (a) $\triangle$ROx, (b) ultraviolet radiation (UV), (c) air temperature (T), (d) wind speed (WS). The y-axis is the smoothing function values. For example, s(UV, df) shows the trend in $\triangle P(O_3)$ when UV changes, and the number of df is the degree of freedom. The x-axis is the influencing factor, and the shaded area around the solid blue line indicates the 95% confidence interval of $\triangle P(O_3)$. The blue vertical short lines represent the distribution characteristics of the explanatory variables (units: $\triangle$ROx ($molecules \cdot cm^{-3}$), UV ($W \cdot m^{-2}$), T (°C), WS ($m \cdot s^{-1}$)).

**Table S1.** Detailed uncertainty and detection limit of instruments used for trace gas observation at the observation site.

**Table S2.** Descriptive statistics of measured VOCs mixing ratios (Units: ppbv).

**Table S3.** Variance inflation factor values quantify the degree of multicollinearity for the PAN influencing factors.

**Table S4.** The measured species and parameters on the inhibition effect stages and promotion effect stages of PAN on $O_3$ in spring and autumn.

## Text 1. Model Validation.

**OBM Model Validation:** The index of agreement (IOA) can be used to judge the reliability of the OBM model simulation results, and its equation is (Liu et al., 2019):

$$IOA = 1 - \frac{\sum_{i=1}^{n}(O_i - S_i)^2}{\sum_{i=1}^{n}(|O_i - \bar{O}| - |S_i - \bar{O}|)^2} \quad (4)$$

where *Si* is simulated value, *Oi* represents observed value, $\bar{O}$ is the average observed values, and n is the sample number. The IOA range is 0-1, and the higher the IOA value is, the better agreement between simulated and observed values is. In many studies, when IOA ranges from 0.68 to 0.90 (Wang et al., 2018), the simulation results are reasonable, and the IOA in our research is 0.88. Hence, the performance of the OBM-MCM model was reasonably acceptable.

**GAM Model Validation:** Figure S1 and S2 show the residual test results of the Generalized Additive Model (GAM) in spring and autumn, respectively. From the residual Q-Q plots (Fig. S1 (a) and Fig. S2 (a)), the points were mostly on a straight line, indicating that the residuals conformed to a normal distribution. Meanwhile, the residual histogram of the model in Fig. S1 (c) and Fig. S2 (c) showed that the residuals were mainly concentrated around 0, which demonstrated the good fitting degree of the model. From the scatter plot of residuals and linear prediction values (Fig. S1 (b) and Fig. S2 (b)), the residuals were randomly distributed. From the scatter plot of the observed values and the fitted values (Fig. S1 (d) and Fig. S2 (d)), the response variables and the fitted values were well matched, and basically showed a "y = x" distribution. Therefore, the fitting effect of this model was good.

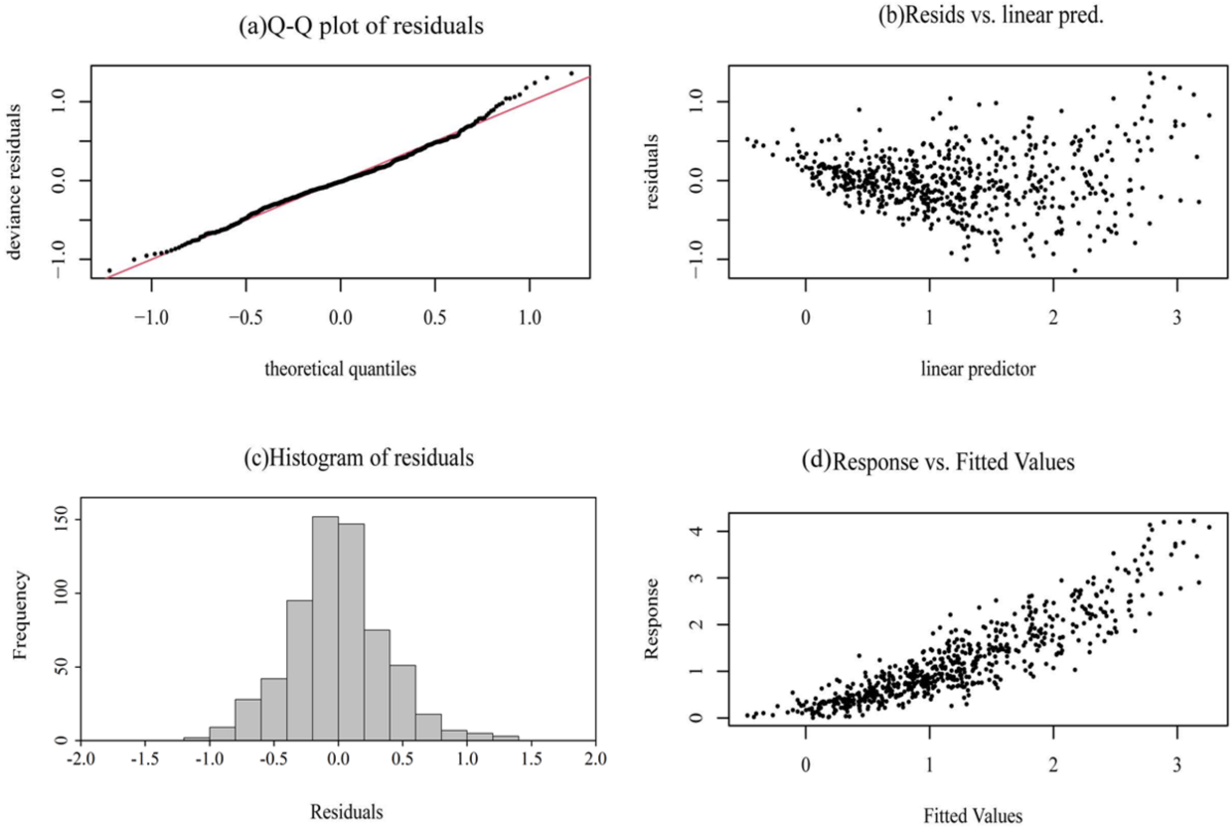


**Figure S1 Residual test results of the Generalized Additive Model (GAM) in spring.**

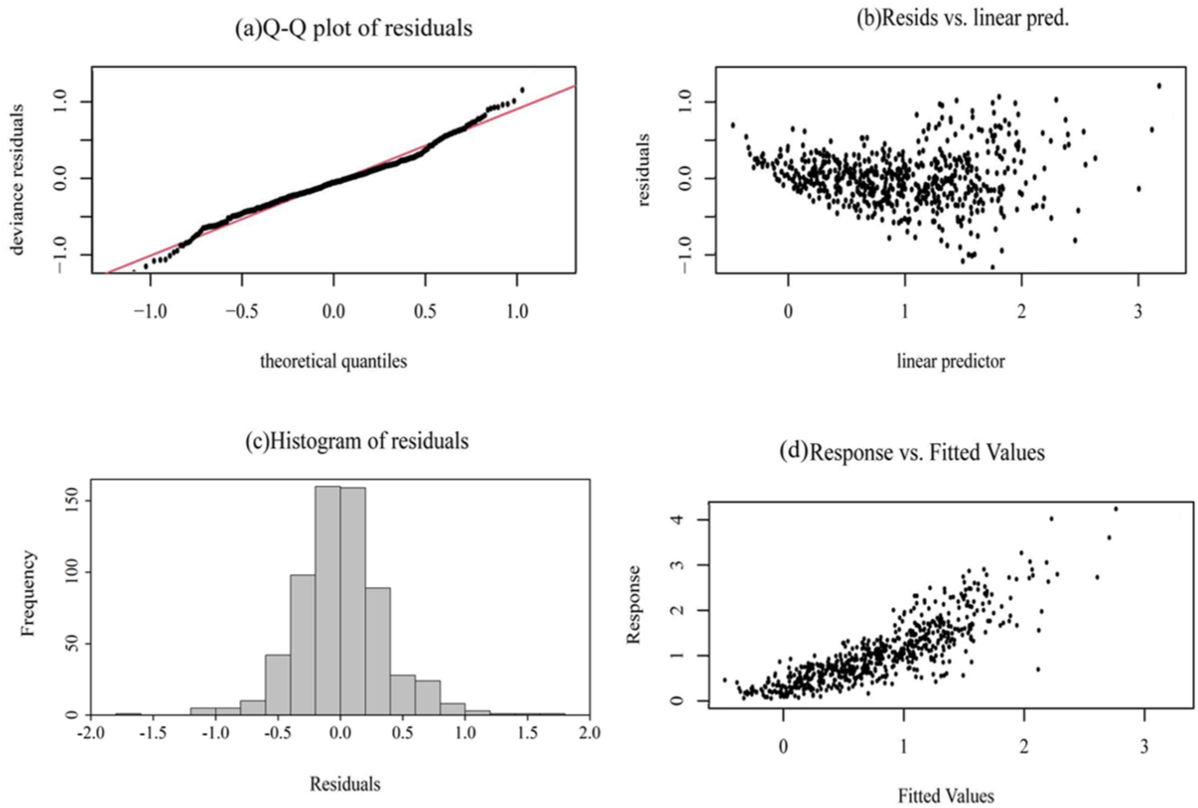


**Figure S2 Residual test results of the Generalized Additive Model (GAM) in autumn.**

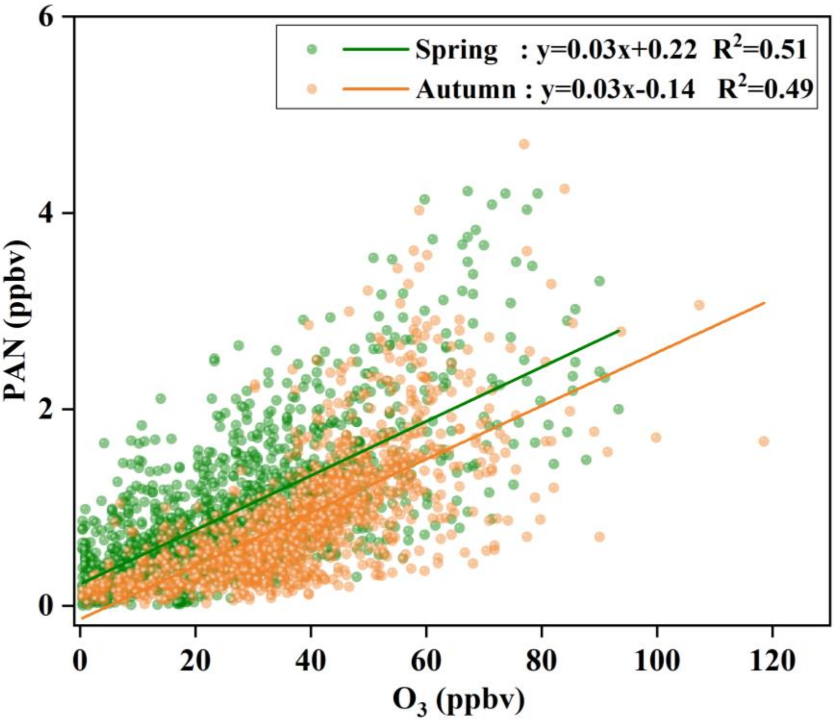


**Figure S3. Scatter plots of PAN versus $O_3$ during the observation periods.**

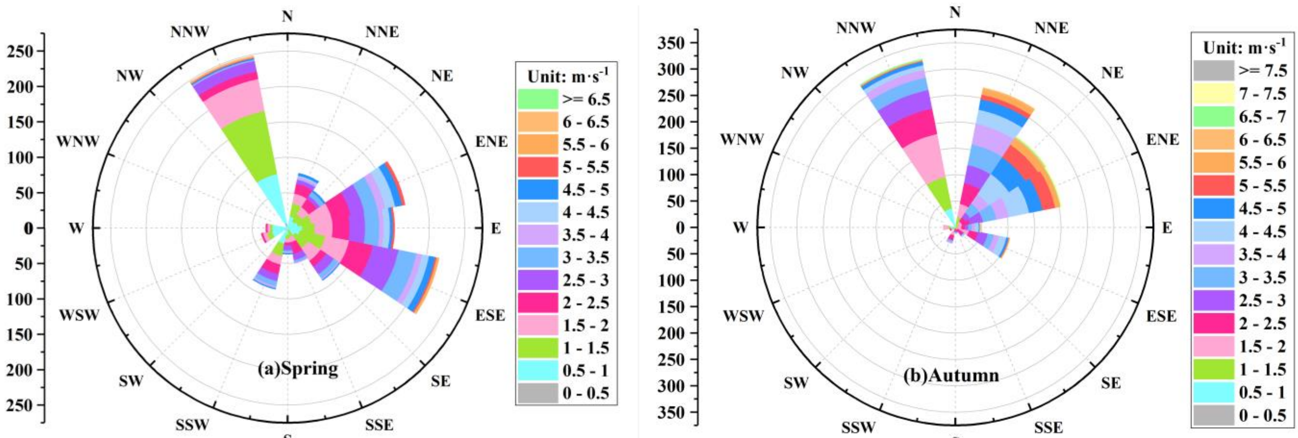


**Figure S4. Wind direction frequency and wind speed plots in (a) spring and (b) autumn during the observation periods.**

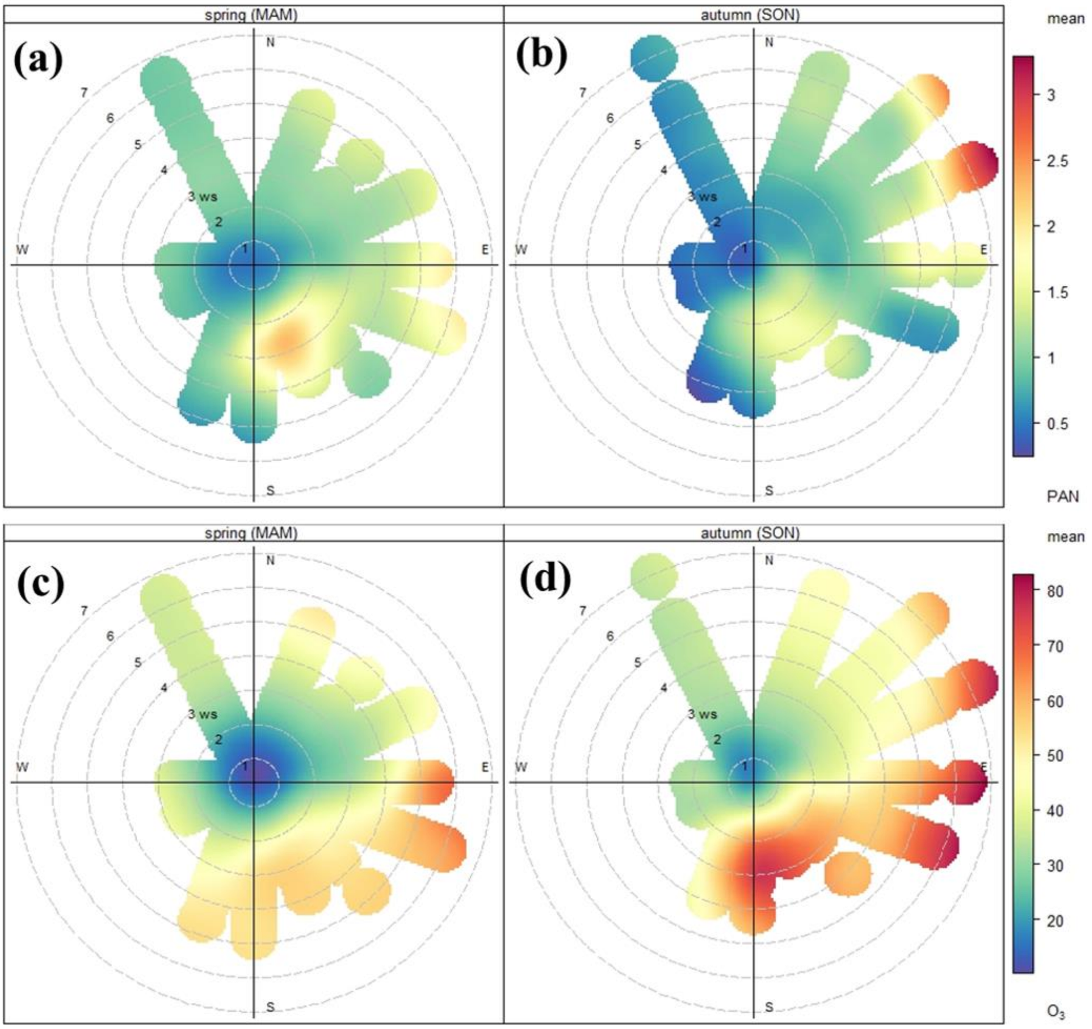


**Figure S5. Bivariate plot of PAN maxing ratios in (a) spring and (b) autumn, and $O_3$ mixing ratios in (c) spring and (d) autumn, respectively (units: ppbv of PAN and $O_3$ maxing ratio, $m \cdot s^{-1}$ of wind speed).**

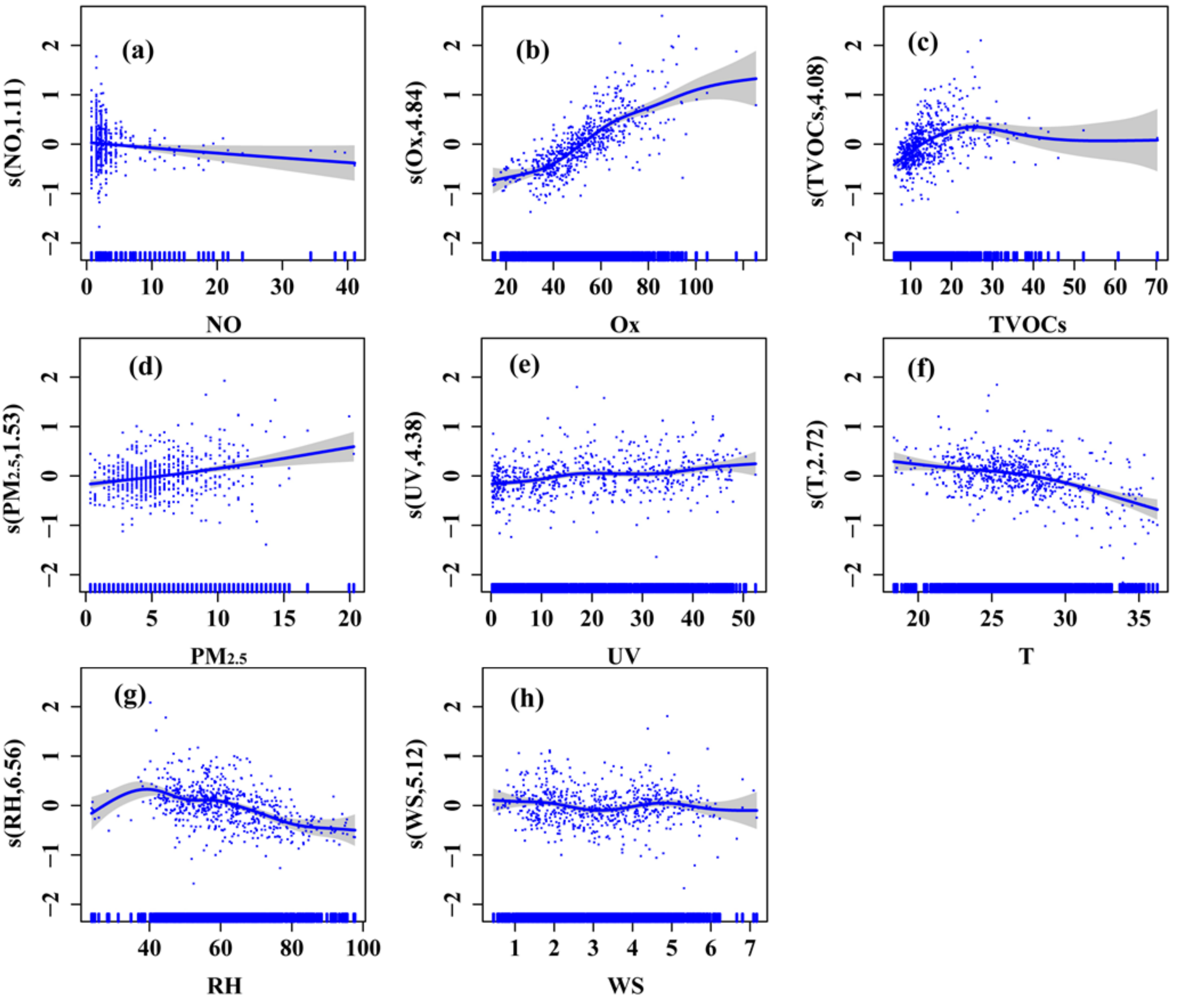


**Figure S6. Response curves (autumn) in the multiple-factor model of PAN mixing ratio to changes in (a) NO, (b) Ox ($Ox=O_3+NO_2$), (c) TVOCs, (d) $PM_{2.5}$ concentration, (e) ultraviolet radiation (UV), (f) air temperature (T), (g) relative humidity (RH), and (h) wind speed (WS). The y-axis is the smoothing function values. For example, s(NO, df) shows the trend in PAN when NO changes, and the number of df is the degree of freedom. The x-axis is the influencing factor, and the shaded area around the solid blue line indicates the 95% confidence interval of PAN. The blue vertical short lines represent the distribution characteristics of the explanatory variables (units: NO (ppbv), Ox ($O_3+NO_2$) (ppbv), TVOCs (ppbv), $PM_{2.5}$ ($\mu g \cdot m^{-3}$), UV ($W \cdot m^{-2}$), T (℃), RH (%), WS ($m \cdot s^{-1}$)).**

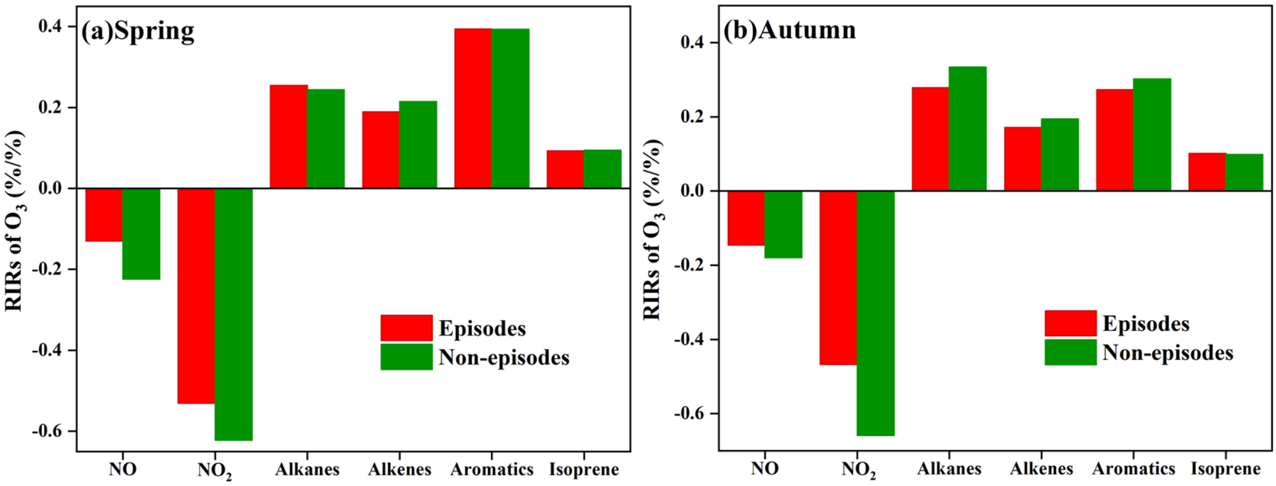


**Figure S7. The OBM-MCM calculated relative incremental reactivity (RIR) for major $O_3$ precursor groups in (a) spring and (b) autumn during the daytime (06:00-17:00 LT) on different pollution scenarios.**

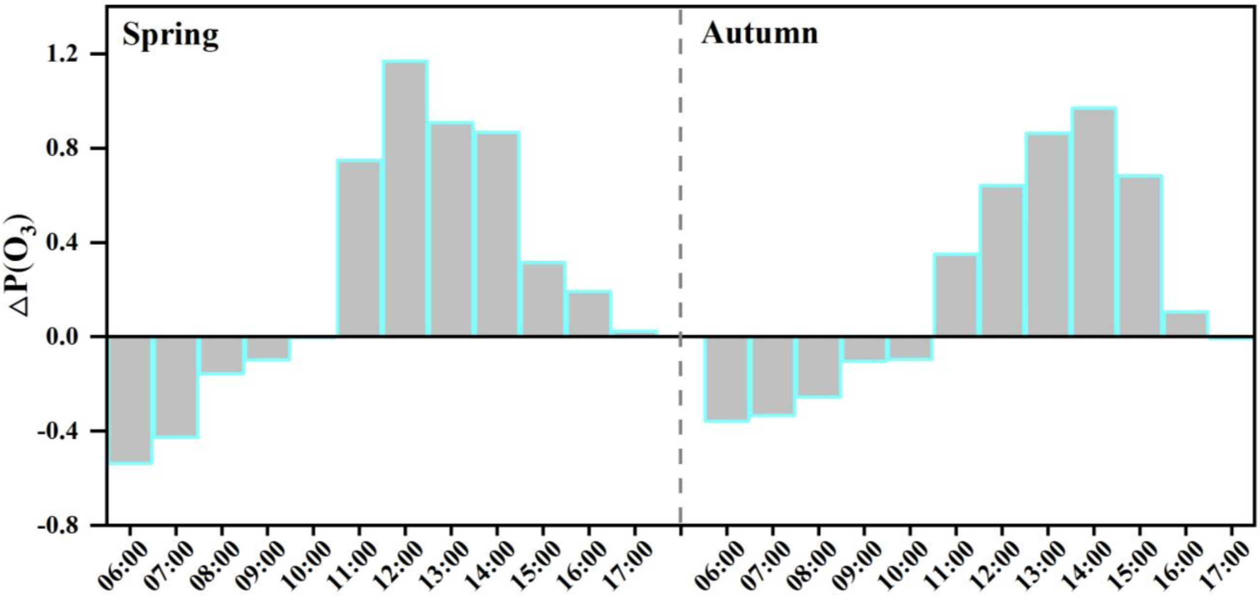


**Figure S8. Diurnal trends of the relative variations of $O_3$ net production $\triangle P(O_3)$ ($ppbv \cdot h^{-1}$) during the daytime in the SC1 to those simulated with PAN chemistry disabled in SC2 during the daytime (06:00-17:00) in (a) spring and (b) autumn (unit: $ppbv \cdot h^{-1}$ for $\triangle P(O_3)$). The data in the picture came from the days that have significant promotion effects of PAN on $O_3$ in spring and autumn.**

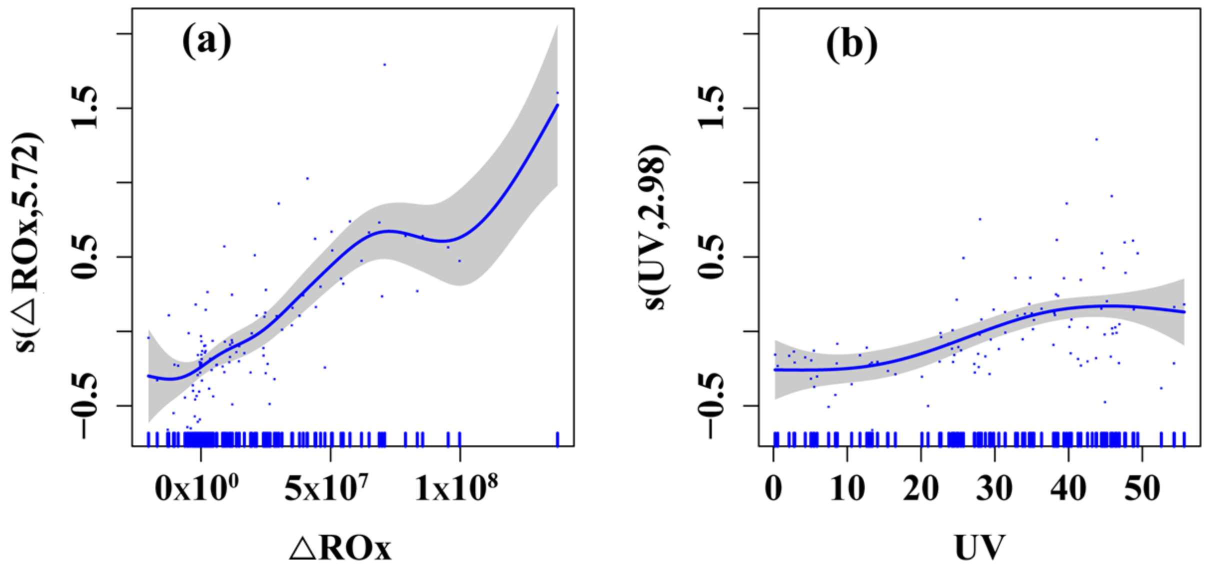


**Figure S9. Response curves (spring) of △P($O_3$) to changes in (a) △ROx, (b) ultraviolet radiation (UV), (f) air temperature (T), (g) relative humidity (RH), and (h) wind speed (WS). The y-axis is the smoothing function values. For example, s(UV, df) shows the trend in △P($O_3$) when UV changes, and the number of df is the degree of freedom. The x-axis is the influencing factor, and the shaded area around the solid blue line indicates the 95% confidence interval of △P($O_3$). The blue vertical short lines represent the distribution characteristics of the explanatory variables (units: △ROx (molecules·$cm^{-3}$), UV (W·$m^{-2}$)).**

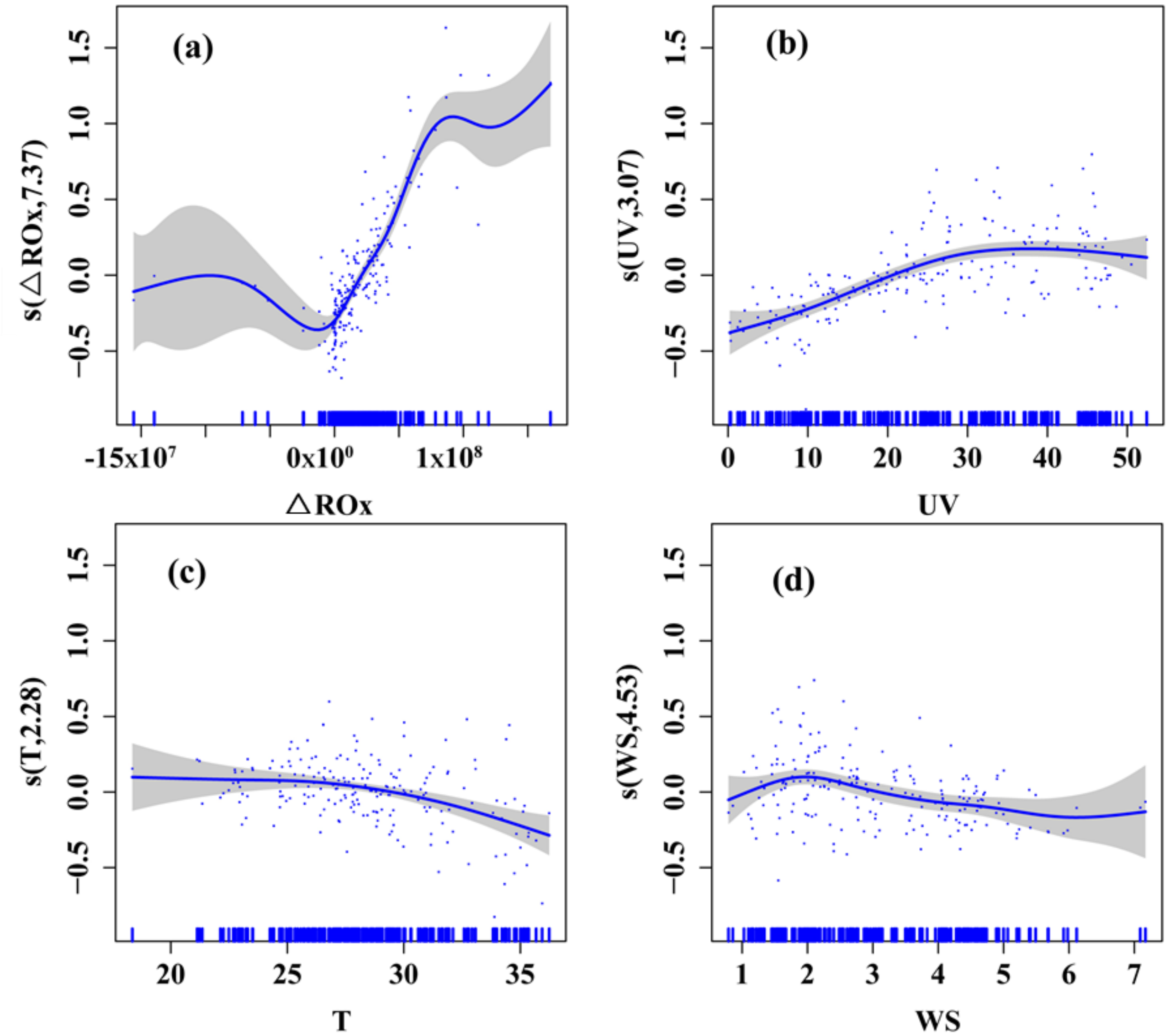


**Figure S10. Response curves (autumn) of △P($O_3$) to changes in (a) △ROx, (b) ultraviolet radiation (UV), (c) air temperature (T), (d) wind speed (WS). The y-axis is the smoothing function values. For example, s(UV, df) shows the trend in △P($O_3$) when UV changes, and the number of df is the degree of freedom. The x-axis is the influencing factor, and the shaded area around the solid blue line indicates the 95% confidence interval of △P($O_3$). The blue vertical short lines represent the distribution characteristics of the explanatory variables (units: △ROx (molecules·$cm^{-3}$), UV (W·$m^{-2}$), T (°C), WS (m·$s^{-1}$)).**

**Table S1. Detailed uncertainty and detection limit of instruments used for trace gas observation at the observation site.**

| Parameter | Experimental Technique | Uncertainty | Detection limit |
|---|---|---|---|
| PAN | PANs-1000, Focused Photonics Inc., Hangzhou, CN | ±10% | 50 pptv |
| $O_3$ | Model 49i, Thermo Fischer Scientific, USA | ±5% | 1 ppbv |
| NOx | Model 42i, Thermo Fischer Scientific, USA | ±10% | 0.5 ppbv |
| CO | Model 48i, Thermo Fischer Scientific, USA | ±5% | 40 ppbv |
| $SO_2$ | Model 43i, Thermo Fischer Scientific, USA | ±10% | 0.5 ppbv |
| VOCs | GC-FID/MS, TH-300B, Wuhan, CN | ±10% | 20-300 pptv |
| HONO | MARGA, ADI 2080, Applikon Analytical B.V., the Netherlands | ±20% | 50 pptv |

**Table S2. Descriptive statistics of measured VOCs mixing ratios (Units: ppbv).**

| Chemicals | Spring | | Autumn | | Chemicals | Spring | | Autumn | |
|---|---|---|---|---|---|---|---|---|---|
| | Mean | SD | Mean | SD | | Mean | SD | Mean | SD |
| **Alkanes** | **9.41** | **5.30** | **5.47** | **2.88** | **Alkyne** | **1.00** | **0.55** | **0.63** | **0.34** |
| Ethane | 2.39 | 1.02 | 1.31 | 0.43 | **Aromatics** | **2.71** | **2.33** | **1.62** | **1.15** |
| Propane | 2.31 | 1.29 | 1.19 | 0.58 | Benzene | 0.27 | 0.14 | 0.16 | 0.09 |
| iso-Butane | 0.87 | 0.57 | 0.52 | 0.37 | Toluene | 1.37 | 1.21 | 0.85 | 0.84 |
| n-Butane | 1.30 | 0.94 | 0.77 | 0.59 | m/p-Xylene | 0.53 | 0.63 | 0.39 | 0.32 |
| iso-Pentane | 1.15 | 1.27 | 0.52 | 0.44 | Ethylbenzene | 0.18 | 0.18 | 0.09 | 0.10 |
| n-Pentane | 0.44 | 0.42 | 0.24 | 0.21 | Styrene | 0.09 | 0.16 | 0.02 | 0.04 |
| 2,2-Dimethylbutane | 0.02 | 0.02 | 0.02 | 0.01 | o-Xylene | 0.19 | 0.23 | 0.04 | 0.09 |
| 2,3-Dimethylbutane | 0.05 | 0.06 | 0.05 | 0.05 | m-Ethyltoluene | 0.02 | 0.02 | 0.01 | 0.01 |
| 2-Methylpentane | 0.08 | 0.09 | 0.05 | 0.04 | 1,3,5-Trimethylbenzene | 0.01 | 0.01 | 0.01 | 0.01 |
| 3-Methylpentane | 0.14 | 0.15 | 0.06 | 0.06 | p-Ethyltoluene | 0.01 | 0.01 | 0.01 | 0.005 |
| n-Hexane | 0.20 | 0.25 | 0.10 | 0.20 | 1,2,4-Trimethylbenzene | 0.03 | 0.05 | 0.01 | 0.02 |
| Cyclohexane | 0.04 | 0.04 | 0.02 | 0.02 | 1,2,3-Trimethylbenzene | 0.01 | 0.01 | 0.01 | 0.004 |
| 2-Methylhexane | 0.05 | 0.06 | 0.04 | 0.05 | **Isoprene (BHC)** | **0.08** | **0.14** | **0.10** | **0.17** |
| 3-Methylhexane | 0.08 | 0.09 | 0.05 | 0.08 | **Halocarbons** | **2.54** | **1.27** | **1.95** | **0.90** |
| n-Heptane | 0.07 | 0.08 | 0.05 | 0.06 | Chloromethane | 0.51 | 0.23 | 0.46 | 0.18 |
| n-Octane | 0.04 | 0.06 | 0.09 | 0.06 | Bromomethane | 0.06 | 0.03 | 0.04 | 0.02 |
| n-Nonane | 0.02 | 0.01 | 0.01 | 0.005 | Dichloromethane | 1.19 | 0.81 | 0.87 | 0.50 |
| n-Decane | 0.01 | 0.01 | 0.01 | 0.01 | Trichloromethane | 0.07 | 0.03 | 0.05 | 0.02 |
| n-Undecane | 0.02 | 0.02 | 0.03 | 0.03 | 1,2-Dichloroethane | 0.51 | 0.34 | 0.36 | 0.22 |
| n-Dodecane | 0.12 | 0.29 | 0.36 | 0.84 | Trichloroethene | 0.02 | 0.02 | 0.02 | 0.01 |
| **Alkenes** | **1.30** | **0.89** | **0.85** | **0.48** | 1,2-Dichloropropane | 0.12 | 0.13 | 0.10 | 0.08 |
| Ethene | 0.90 | 0.65 | 0.51 | 0.34 | Tetrachloroethene | 0.05 | 0.05 | 0.04 | 0.05 |
| Propene | 0.20 | 0.14 | 0.19 | 0.11 | **OVOCs** | **4.49** | **1.83** | **4.17** | **2.57** |
| 1-Butene | 0.04 | 0.03 | 0.03 | 0.02 | Acrolein | 0.06 | 0.03 | 0.04 | 0.02 |
| cis-2-Butene | 0.05 | 0.06 | 0.03 | 0.03 | Acetone | 2.22 | 0.94 | 2.21 | 0.91 |
| trans-2-Butene | 0.03 | 0.06 | 0.03 | 0.02 | 2-Butanone | 0.67 | 0.45 | 0.50 | 0.44 |
| 1-Pentene | 0.02 | 0.02 | 0.01 | 0.01 | 2-Propanol | 0.24 | 0.31 | 0.12 | 0.12 |
| trans-2-Pentene | 0.04 | 0.04 | 0.04 | 0.02 | 2-Methoxy-2-methylpropane | 0.24 | 0.32 | 0.09 | 0.09 |
| 1,3-Butadiene | 0.01 | 0.02 | 0.01 | 0.01 | Ethylacetate | 1.07 | 0.83 | 1.20 | 1.31 |

**Table S3. Variance inflation factor values quantify the degree of multicollinearity for the PAN influencing factors.**

| Smooth variable | NO (ppbv) | Ox ($O_3$+$NO_2$) (ppbv) | TVOCs (ppbv) | $PM_{2.5}$ ($\mu g \cdot m^{-3}$) | UV ($W \cdot m^{-2}$) | T (℃) | RH (%) | WS ($m \cdot s^{-1}$) |
|---|---|---|---|---|---|---|---|---|
| Spring | 1.437 | 3.512 | 1.88 | 1.545 | 1.815 | 1.62 | 3.5 | 1.75 |
| Autumn | 1.345 | 2.276 | 1.732 | 1.532 | 1.232 | 1.806 | 2.098 | 1.769 |

**Table S4. The measured species and parameters on the inhibition effect stages and promotion effect stages of PAN on $O_3$ in spring and autumn.**

| Parameters | Spring | | | | Autumn | | | |
|---|---|---|---|---|---|---|---|---|
| | Inhibition | | Promotion | | Inhibition | | Promotion | |
| | Mean | SD | Mean | SD | Mean | SD | Mean | SD |
| PAN (ppbv) | 1.04 | 0.74 | 1.89 | 1.00 | 0.84 | 0.53 | 1.58 | 0.70 |
| $O_3$ (ppbv) | 27.32 | 18.02 | 50.26 | 25.77 | 36.42 | 16.26 | 53.51 | 16.63 |
| NO (ppbv) | 6.31 | 9.76 | 4.06 | 7.82 | 3.42 | 4.36 | 2.70 | 3.50 |
| $NO_2$ (ppbv) | 13.08 | 7.38 | 8.55 | 6.31 | 10.23 | 5.43 | 9.46 | 5.74 |
| CO (ppbv) | 302.84 | 69.10 | 283.35 | 62.22 | 252.85 | 52.89 | 239.44 | 46.55 |
| $SO_2$ (ppbv) | 2.36 | 1.14 | 2.66 | 1.32 | 3.24 | 0.68 | 3.20 | 0.91 |
| UV ($W \cdot m^{-2}$) | 15.40 | 13.95 | 29.76 | 14.84 | 17.68 | 14.07 | 24.95 | 13.72 |
| T (°C) | 21.57 | 4.13 | 26.69 | 4.22 | 25.95 | 3.08 | 28.39 | 3.50 |
| RH (%) | 70.62 | 16.31 | 56.77 | 17.13 | 63.77 | 13.22 | 54.45 | 9.94 |
| P (hPa) | 1010.08 | 3.65 | 1008.24 | 3.50 | 1008.92 | 3.58 | 1007.61 | 3.67 |
| Wind speed ($m \cdot s^{-1}$) | 2.01 | 1.10 | 2.83 | 1.22 | 3.18 | 1.44 | 3.08 | 1.35 |
| $PM_{2.5}$ ($\mu g \cdot m^{-3}$) | 9.23 | 5.45 | 9.67 | 4.68 | 5.40 | 3.00 | 5.94 | 3.15 |
| TVOCs (ppbv) | 23.55 | 10.45 | 17.51 | 6.78 | 15.25 | 8.11 | 13.29 | 5.03 |

## Reference:


Wang, Y., Guo, H., Zou, S., Lyu, X., Ling, Z., Cheng, H., and Zeren, Y.: Surface $O_3$ photochemistry over the South China Sea: Application of a near-explicit chemical mechanism box model, Environ. Pollut., 234, 155–166, https://doi.org/10.1016/j.envpol.2017.11.001, 2018.

Liu, J., Wang, L., Li, M., Liao, Z., Sun, Y., Song, T., Gao, W., Wang, Y., Li, Y., Ji, D., Hu, B., Kerminen, V.-M., Wang, Y., and Kulmala, M.: Quantifying the impact of synoptic circulation patterns on ozone variability in northern China from April to October 2013–2017, Atmos. Chem. Phys., 19, 14477–14492, https://doi.org/10.5194/acp-19-14477-2019, 2019.